Dechlorination of *p*-Chlorophenol in a Microreactor with Bimetallic Pd/Fe Catalyst

Goran N. Jovanovic,*,† Polona Žnidaršič Plazl,‡ Ploenpun Sakrittichai,† and Khaled Al-Khaldi†

Department of Chemical Engineering, Oregon State University, 103 Gleeson Hall, Corvallis, Oregon 97331, and Department of Chemical Engineering, Faculty of Chemistry and Chemical Technology, University of Ljubljana, 1000 Ljubljana, Slovenia

Dechlorination of *p*-chlorophenol was investigated in a single-pass, continuous-flow microreactor system made of two parallel palladized iron plates. The plates formed a microscale channel 27 mm wide, 70 mm long, and 0.2 mm high. The bimetallic catalyst was prepared by electroless deposition of Pd on the reactor plate surfaces. Experiments were performed under steady-state conditions at different temperatures between 293 and 333 K and at a variety of flow conditions in the range from 1.5×10^{-9} to 1×10^{-8} m^3/s. A two-dimensional mathematical model, containing convection, diffusion, and pseudo-first-order catalytic reaction terms, was developed to analyze the experimental data and to forecast reactor performance. Depending on the prevailing kinetic and convection/diffusion phenomena, the developed model can be reduced to the ideal plug-flow model or can depict reactor performance that is close to or even worse than the performance of an ideal mixed-flow reactor. Under operating conditions typical to this study, the model and the experimental data indicate plug-flow behavior of the microreactor. Analysis of the obtained chemical kinetic rate constants provides an estimate of the activation energy for this reaction ($E_a = 48.43 \pm 6.13$ kJ/mol), which remains unchanged despite observed deactivation of the catalyst. The deactivation of the catalyst is caused by reversible catalyst passivity, and it is modeled by second-order kinetics. Analysis of the experimental data shows that the observed deactivation influences only the preexponential factor in the Arrhenius law for the investigated reaction.

Introduction

Chlorophenols, a major group of pollutants used extensively in pesticides, fungicides, herbicides, dyes, and solvents, are causing great environmental concern because of their toxicity and resistance to degradation.[1] Widespread contamination of water supplies with chlorinated solvents and pesticides has spurred an intense effort to find efficient and cost-effective treatment. In addition to conventional technologies, such as air stripping and granular activated carbon treatments, several types of catalytic chemical degradations, biological remediations, and photochemical decompositions of chlorocarbons have been reported.[2−6]

The metal-enhanced catalytic dechlorination process is one of the most attractive methods for solving the ecological problems related to contamination with chlorinated compounds. Catalytic dechlorination has an advantage over other processes because it eliminates chlorinated hydrocarbons instead of just moving them into another phase or medium (as done, for example, in activated carbon adsorption, thermal desorption, and vitrification).

In addition to catalytic hydrodechlorination,[2,3] bimetallic catalysis, along with the electrochemical method, provides very efficient dechlorination because of its ability to thoroughly purify a wide range of chlorinated compounds without leaving chlorinated side products (as is often the case for bioremediation or use of zerovalent iron alone[4−10]). The most frequently used catalysts are Pd, Ni, Rh, and Pt. These are supported on Fe, graphite, or highly porous metallic oxides such as Al_2O_3. The Pd/Fe catalytic system has gained much attention, because it is highly reactive and because it can be implemented in a number of forms, including palladized iron wire,[4] impregnated iron particles,[5−12] palladized iron plates,[13] and alginate-entrapped catalyst.[6,11] Different forms of Pd/Fe catalyst have successfully been used to treat a wide range of chlorinated compounds, including chlorophenols,[4−6,9,11,12] polychlorinated biphenyls,[7−10] and chlorinated aliphatic compounds.[10,12]

The chlorinated compounds that are adsorbed on the bimetallic surface are reductively dechlorinated through a series of reactions. According to Graham and Jovanovic,[6] the chemical process involved in the *p*-chlorophenol dechlorination reaction on Pd/Fe catalyst encompasses three sets of chemical reactions, namely, surface reactions (eqs 1−3), solution reactions (eqs 4 and 5), and the actual chlorine removal reaction (eq 6), as listed below and schematically presented in Figure 1

Surface reactions

$$Fe^0 \rightarrow Fe^{2+} + 2e^- \quad (1)$$

$$2H^+ + 2e^- \xrightarrow{Fe} H_2(g) \quad (2)$$

$$H^+ + e^- \xrightarrow{Pd} H^* \quad (3)$$

* To whom correspondence should be addressed. Tel.: 541 737 3614. Fax: 541 737 4600. E-mail: goran@engr.orst.edu.
† Oregon State University.
‡ University of Ljubljana.

10.1021/ie049496+ CCC: $30.25
Published on Web 12/31/2004

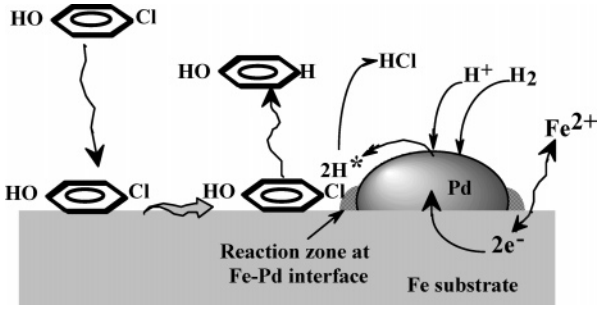

Figure 1. Graphical presentation of multistep dechlorination process on the Pd/Fe catalyst surface.

Solution reactions

$$2H_2O \rightarrow 2H^+ + 2OH^- \quad (4)$$

$$2HCl \rightarrow 2H^+ + 2Cl^- \quad (5)$$

Dechlorination reaction

$$2H^* + R{-}Cl \rightarrow R{-}H + HCl \quad (6)$$

The overall dechlorination reaction process on Pd/Fe catalyst can be represented as

$$Fe^0 + R{-}Cl + H^+ \rightarrow R{-}H + Fe^{2+} + Cl^- \quad (7)$$

These reactions are found to be dependent on several parameters, including the pH, the Pd/Fe interface area, the extent of palladization, the ratio of the Pd/Fe interfacial area to the amount of chlorine to be removed, and the amount of dissolved oxygen.[6,11]

Furthermore, reactions and phenomena related to catalyst deactivation are also of concern. In previous studies,[6,11,13] appreciable deactivation was observed after extended use of catalysts, typically after several hours of continuous reaction. The deactivation process is introduced by any of the following three causes, graphically illustrated in Figure 2: loss of catalyst base (i.e., dissolution of Fe into the liquid solution), iron hydroxide precipitation, and extensive hydrogen gas formation. Formations of an iron hydroxide layer and a H_2 gas blanket are reversible processes, and they result in to temporary catalyst passivity. Both processes can be successfully suppressed by an aggressive pH control in a deoxygenated environment, as demonstrated previously.[6,11]

Microtechnology has uncovered new scientific solutions and challenges in a broad range of areas, from electronics, medical technology, and fuel production and processing to biotechnology, the chemical industry, environmental protection, and process safety. Because of the small amounts of chemicals needed and the high rate of heat and mass transfer, microscale systems are especially suited for reactions with highly toxic, flammable, and explosive reactants.[14,15] In the area of catalytic chemistry, microreactors are an extremely efficient tool for rapid catalyst screening and for combinatorial chemistry.[16] Moreover, the small length scale of microreactors reduces transport limitations, giving nearly gradientless conditions desirable for the determination of reaction kinetics.[17,18] In the past few years, several papers have discussed the field of miniaturization of catalytic reactors.[19−21]

However, relatively few studies in this area have investigated heterogeneously catalyzed liquid-phase reaction processes in microscale reactors. A few examples, reviewed by Jähnisch et al.,[14] indicate a 10% to severalfold increase of reaction yield when compared to conventional reactor processes. Recently, the first study of an enzymatic reaction in two-phase flow in a microfluidic device was reported by Maruyama et al.,[22] where degradation of *p*-chlorophenol was realized by solubilized laccase.

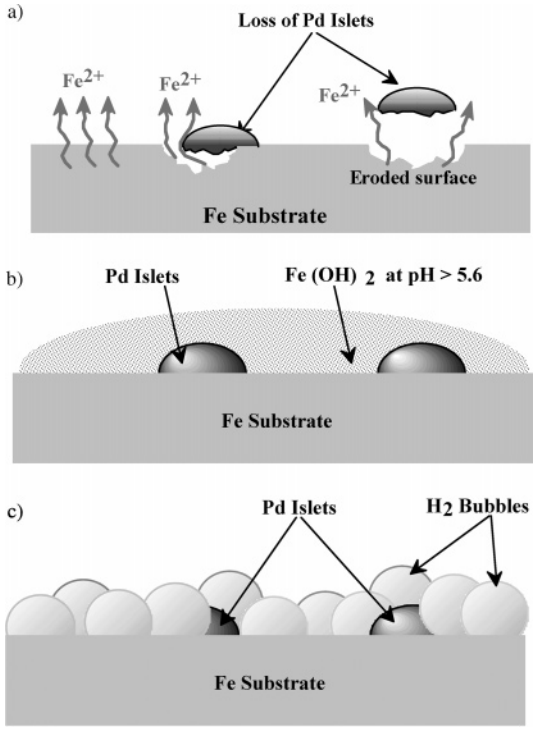

Figure 2. Illustration of catalyst deactivation due to (a) loss of catalyst base, i.e., dissolution of Fe into the liquid solution; (b) iron hydroxide precipitation; and (c) extensive hydrogen gas formation.

In our study, the use of a microreactor for the degradation of *p*-chlorophenol on bimetallic Pd/Fe catalyst is presented, which has a potential use in on-site pollutant remediation. The goal of the study is to obtain the dechlorination of *p*-chlorophenol in a continuous-flow microreactor made of two iron plates palladized by electroless deposition of Pd on the reactor plate surfaces. A mathematical model is developed to describe and predict reactor performance at steady-state conditions. Microreactor simulations are compared with ideal plug-flow reactor (PFR) and continuous stirred-tank reactor (CSTR) models for a broad range of operating conditions. Furthermore, the deactivation of catalyst that resulted in unsteady-state operation is described by a dynamic model. Finally, an estimate of the activation energy for this reaction is obtained.

Experimental Section

Materials. Pure iron (TW Metals) was used as the plating substrate for the Pd catalyst. A powdered form of $PdCl_2$ (59% Pd, Acros Organics) was dissolved in deionized water to yield 1 mM solution. A solution of *p*-chlorophenol (>99% purity, Aldrich) in deionized water was used as the reactant in a process of dechlorination, and a 1000 ppm phenol solution (98.5% purity, Fischer Scientific) was used as the standard for product determination. Acetic acid, HCl, and HPLC-grade methanol were obtained from Fischer Scientific.

Catalyst Preparation. Prior to palladization, iron plates ($W = 27 \pm 0.0002$ mm and $L = 70 \pm 0.001$ mm)

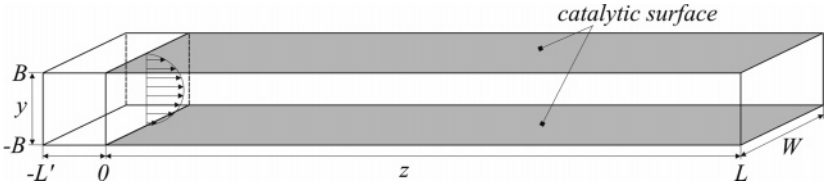

Figure 3. Apparatus for steady-state dechlorination. The positive-displacement pump drives a well-mixed reactant solution from the feed container through the microreactor, and the samples are withdrawn at the outlet and analyzed off-line by HPLC.

were immersed in 1 M HCl to remove any foreign metals that might have been picked up during mechanical preparation and to remove surface oxide layers. After a thorough rinsing of the plates with deionized water, two iron plates were attached to a polypropylene mounting disk. The electroless plating of Pd was performed by immersion in a disk-coating bath with a solution of 1 mM $PdCl_2$ and 0.1 M HCl, and the disk was rotated at 300 rpm unless the dark orange $PdCl_2$ solution turned colorless. The procedure was always performed under exactly the same conditions to ensure the deposition of the same amount of Pd and to achieve the same surface quality on each plate. After the palladization, the iron plates were rinsed with deionized water and kept for later use without drying.

Apparatus and Experimental Procedure. The experimental apparatus for steady-state dechlorination is shown in Figure 3. A pair of palladized iron plates attached to polypropylene disks was used in the microreactor, which was housed in a stainless steel casing, 0.152 m in diameter and 0.019 m thick, with an empty reactor volume of 1.2 mL. The space between the plates (maximum depth of 200 ± 1.02 μm) acted as a flow channel. A Pd catalyst loading of 20 mg (10 mg per plate) was used to dechlorinate *p*-chlorophenol, which was prepared as a 100 ppm (7.8×10^{-7} mol/m^3) aqueous solution and sparged with pure N_2 to remove dissolved oxygen. The pH of the solution was adjusted to 5.3 by HCl addition. The reactant solution was pumped through a tightly closed reactor by a positive-displacement pump in downstream configuration at a constant flow rate in the range from 0.09 to 0.63 (±0.002) mL/min. The mean residence time of fluid in the reactor was between 2 and 12 min over the operating range of flow rates used. All tubing was made of PTFE (polytetrafluoroethylene), and nylon was used for all fittings. The reactor was first placed in a vertical position to eliminate the formation of gas pockets, which might cause the presence of air bubbles in the samples. The experiments were conducted for 24 h at temperatures in a range between 293 and 333 K, where the temperatures of both the inlet line and the reactor itself were kept constant.

Analyses. The amount of deposited Pd catalyst was calculated from the concentrations of the $PdCl_2$ solution, estimated spectrophotometrically at 480 nm, before and after electroless plating. An Amray 3300FE scanning electron microscope was used to produce micrographs of the Pd/Fe catalyst surface.

The concentrations of *p*-chlorophenol and phenol were assayed using HPLC with a 5-μ, LC-8 column (Supelco). Elution was obtained with a mobile phase consisting of 60 vol % acetic acid/methanol solution (1:99 vol %) and 40 vol % acetic acid/deionized water solution (1:99 vol %) at a flow rate of 1.0 mL/min. Absorbance detection was at 254 nm, and the *p*-chlorophenol and phenol concentrations were determined from calibration curves obtained with standard solutions.

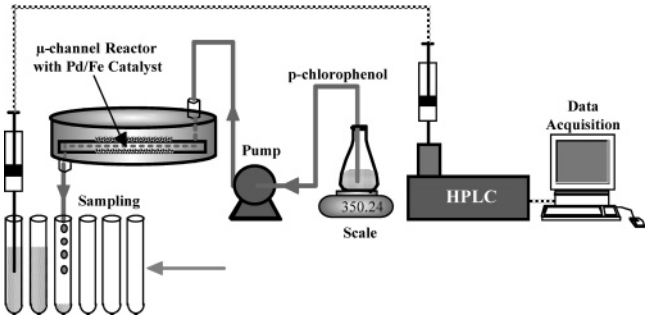

Figure 4. Schematic presentation of the microreactor system, in modeling separated into two parts to consider back-mixing in front of the catalytic zone ($-L' \le z \le 0$). Microreactor dimensions: L = 70 mm, W = 27 mm, and B = 0.1 mm.

Mathematical Modeling

For dechlorination in a microreactor with laminar fluid flow, a two-dimensional (2D) model is developed. Both longitudinal and transverse diffusion and convection in the longitudinal direction are considered, with an irreversible, pseudo-first-order reaction at the catalyst surfaces on both sides of the flow channel. For an accurate description of the effects of back-mixing at the inlet of the catalytic area ($z = 0$), the precatalytic zone is considered, as shown in Figure 4. In this zone, which represents a defined portion of the system (L' is approximately $0.1L$), the boundary conditions without chemical reaction are taken into account.

For steady-state conditions in the single-pass microreactor system before catalyst deactivation, the dimensionless partial differential equation is

$$(1 - \psi^2)\frac{\partial X}{\partial \xi} = \frac{D_{AB}}{B v_m}\left(\frac{\partial^2 X}{\partial \xi^2} + \frac{\partial^2 X}{\partial \psi^2}\right) \tag{8}$$

with the boundary conditions

$$X\left(-\frac{L'}{B},\psi\right) = X_0, \qquad -1 \le \psi \le 1$$

$$\frac{dX}{d\xi}\left(\frac{L}{B},\psi\right) = 0 \qquad -1 \le \psi \le 1$$

and

$$-D_{AB}(W\,d\xi)\left.\frac{dX}{d\psi}\right|_{\xi=\pm 1} = \begin{cases} 0 & -\dfrac{L'}{B} \le \xi \le 0 \\ -(W\,d\xi)k^*B\,X, & 0 \le \xi \le \dfrac{L}{B} \end{cases}$$

Dimensionless variables are defined as $\psi = y/B$, $\xi = z/B$, and $X = C_A/C_{A0}$, where y and z are coordinates in the directions of the reactor height and length, respectively, and B represents the half-height of the microreactor. C_A and C_{A0} are the concentrations of *p*-chlorophenol solutions, with 0 denotating the input concentration. The molecular diffusion coefficient for *p*-chloro-

phenol in water, D_{AB}, is calculated at different temperatures using the estimation for nonelectrolytes in liquids at low concentrations.[23] For a fully developed velocity profile in a microchannel, the maximum velocity, v_m, is related to the velocity in the z direction, v_z, by $v_z = v_m(1 - \psi^2)$.

For the catalytic reaction taking place on both parallel plates of catalyst, a previously defined kinetics is used[6]

$$-r_A = (k' w_{cat} C_{H^*}) C_{A0} X = k'' C_{A0} X \tag{9}$$

where the combination of constant k' with C_{H^*}, the concentration of the reactive intermediate H* due to maintenance of constant pH during the process, yields $k = k' C_{H^*}$, and further grouping with the catalyst weight, w_{cat}, gives an overall rate constant k''. Normalization of this constant with respect to the characteristic dimensions of the catalyst yields k^*, where $k^* = k''/WL$ and the overall reaction rate is

$$-r_A = WLk^* C_{A0} X \tag{10}$$

For the numerical solution of the model equations, a finite-difference method was used. Regarding a wide range of theoretical operating conditions, varying nodal densities of meshes were applied. To achieve stability of the system at high Peclet number, Pe, the microreactor was divided into several parts along the reactor length, where each outlet profile served as the input for the next section. On the contrary, at Pe values below 0.1, where a lower nodal density is sufficiently accurate, the whole microreactor was treated as a unit. Using the implicit approach, matrices up to $10^5 \times 10^5$ were solved using the Mathematica 5.0 computational tool.

To describe the deactivation process observed in experimental studies, the activity term a was added to the reaction rate equation, which accounts for the passivation effects, as presented in Figure 2

$$-r_A = k'' C_{A0} X a \tag{11}$$

The activity of the catalyst can be described by an nth-order rate equation[24]

$$-\frac{da}{dt} = k_d a^n \tag{12}$$

where k_d is the deactivation rate coefficient.

From the dynamic model for plug-flow reactor in eqs 11 and 12 and the experimental data after the stationary phase, when deactivation started (at time t_s), the order of the deactivation process and the deactivation rate coefficient were evaluated.

Results and Discussion

Using a wide range of theoretical operating conditions, a dimensionless concentration was calculated for the plug-flow reactor (PFR) model, the continuous stirred-tank reactor (CSTR) model, and our 2D model. The steady-state mass balance of p-chlorophenol dechlorination is given by

$$\frac{C_A}{C_{A0}} = e^{-k^* L / v_{av} B} \tag{13}$$

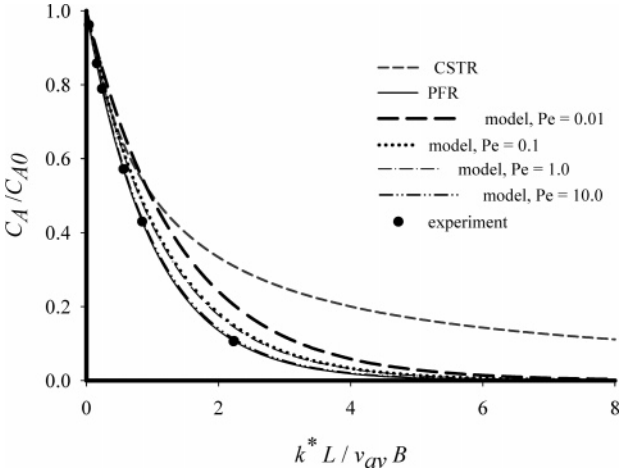

Figure 5. Comparison of the predictions of ideal PFR and CSTR models together with our model simulations for a wide range of theoretical operating conditions, expressed as different Peclet numbers ($0.01 \le Pe \le 10$). The calculations at experimental conditions are also presented (●), where the first three points along the x axis represent experiments at room temperature and at different flow rates of p-chlorophenol solution, whereas further points indicate the experiments at increasing temperatures.

for the PFR and by

$$\frac{C_A}{C_{A0}} = \left(\frac{k^* L}{v_{av} B} + 1\right)^{-1} \tag{14}$$

for the CSTR. Both contain the characteristic dimensionless group $k^*L/v_{av}B$ as an independent parameter for reactor efficiency. Figure 5 compares the predictions for the ideal PFR and CSTR models with our model simulations for different Peclet numbers ($0.01 \le Pe \le 10$) and shows the results obtained in the experiments.

Generally, an increase in the flow rate results in an increase in Pe, and consequently, our model for the microreactor approaches that for a PFR. At $Pe = 10$, the model gives close-to-ideal PFR performance, and a further increase in Peclet number results in the complete overlapping of the model simulations with the PFR curve, so the results are not presented. As the experimental Pe values (based on average axial velocity v_{av}, reactor half-height B, and the molecular diffusivity D_{AB}) were between 17.5 and 223.5 for the whole set of experiments, the results of the model simulations completely match those of the PFR. Similar findings were recently reported by Deshmukh et.al.,[25] who compared a 2D computational fluid dynamic simulation of a complex structured post microreactor with various reactor models. For a wide range of temperatures and flow rates, nearly PFR behavior was observed in the model simulations of a microstructured reactor used for hydrogen production from ammonia.

Only in the case of very low velocities, expressed as Pe values below 1, does the microreactor shift away from PFR behavior, and at very low values of $k^*L/v_{av}B$, it performs even worse than a CSTR (Figure 5). This phenomenon might be explained by pronounced backmixing present at slower flows, not taken into account in the PFR model. In the case of very slow reaction kinetics, this results in lower conversions as compared to those obtained at higher flow rates, where the backmixing from longitudinal diffusion is diminished.

Figure 6 presents results of a 2D model simulation of the dimensionless concentration profile in the first

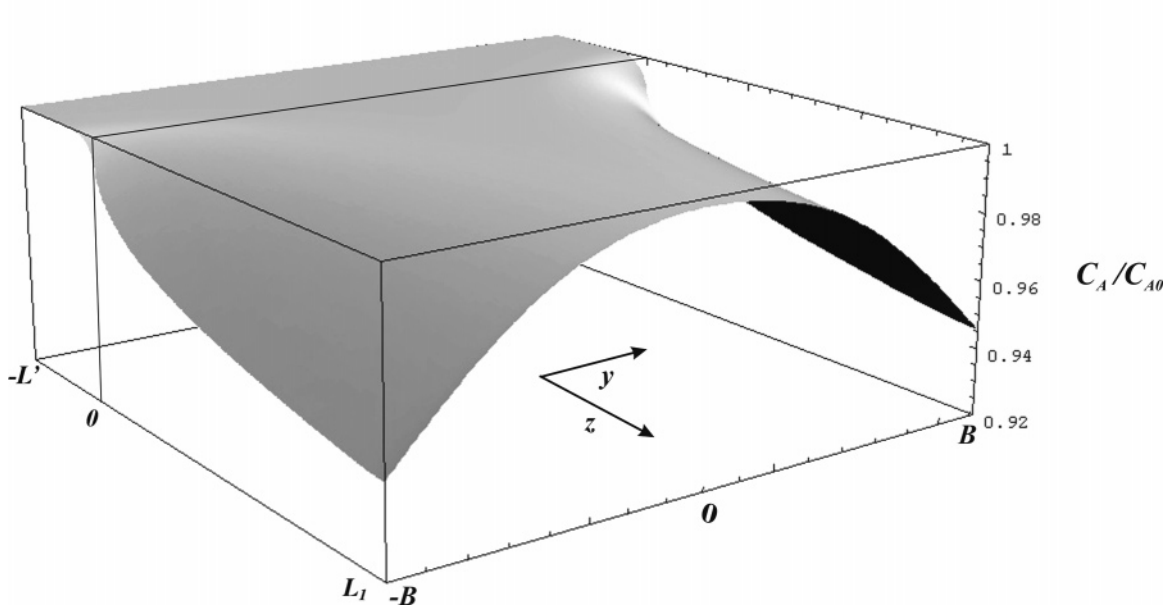

Figure 6. Dimensionless concentration profile at the beginning of the microreactor, including the precatalytic region ($-L' \le z \le 0$) and the first part of catalytic zone ($0 \le z \le L_1$), which accounts for 1/140 of the length of the catalyst.

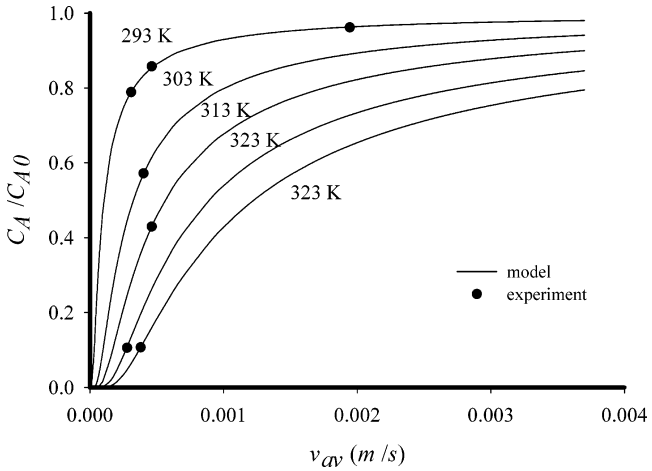

Figure 7. Results of experiments (●) performed at different temperatures (293−333 K) and at different flow rates of *p*-chlorophenol solution in comparison with 2D model predictions (—).

part of the microreactor. A symmetric concentration profile is evident along reactor height because the reaction is taking place on the catalyst on both sides of the microchannel. In the precatalytic region ($-L' \le z \le 0$), a slow decrease in reactant concentration is already observed, resulting from the previously discussed backmixing in the reactor.

The use of Pd/Fe catalyst in the microreactor yielded phenol as the only product of *p*-chlorophenol dechlorination. The ambient-temperature experiments were performed at flow rates from 0.09 to 0.63 mL/min, resulting in Reynolds numbers between 0.12 and 0.77, based on the average axial velocity v_{av}, equilibrium length d_e, fluid density ρ, and viscosity μ. This is in agreement with the laminar flow condition applied in the development of the mathematical model. As seen in Figure 7, the model accurately predicts the conversion of *p*-chlorophenol at different flow rates and yields the corresponding overall rate constant $k^*_{293\,K} = 1.04 \times 10^{-7}$ m/s. Considering the catalyst dimensions, calculation of the rate constant gives $k_{293\,K} = 1.97 \times 10^{-5}$ m^3/kg$_{cat}$·s, which is 3 orders of magnitude lower than the constant reported for granular Pd/Fe catalyst at the same temperature ($k_{293\,K} = 6.52 \times 10^{-2}$ m^3/kg$_{cat}$·s).[6] Another study of *p*-chlorophenol dechlorination with powdered Pd/Fe catalyst at 301 K[5] revealed a constant of $k_{301\,K} = 3.90 \times 10^{-4}$ m^3/kg$_{cat}$·s, and the dechlorination of polychlorinated biphenyls (PCBs) and trichloroethene (TCE) with nanoscale Pd/Fe catalyst[10] yielded $k_{295\,K} = 9.3 \times 10^{-4}$ m^3/kg$_{cat}$·s, which is more similar to our results. The discrepancies in reaction rates are most likely a consequence of the different catalyst sizes and structures. This was also suggested by Zhang et al.,[12] who reported average rate constants for the degradation of *trans*-dichloroethene (*trans*-DCE) varying between $k_{295\,K} = 9.3 \times 10^{-5}$ m^3/kg$_{cat}$·s for nanoscale Pd/Fe particles and $k_{295\,K} = 9.3 \times 10^{-7}$ m^3/kg$_{cat}$·s for microscale iron particles. The comparison of reaction rate constants is summarized in Table 1. From Figure 7, it is evident also that an increase in flow rate, and therefore a decrease in contact time, lowers the conversion of *p*-chlorophenol on Pd/Fe catalyst.

Moreover, the effect of temperature on the dechlorination kinetics was studied at temperatures between 293 and 333 K. As expected, the rate of dechlorination increased at higher temperature to achieve $k^*_{333\,K} = 1.21 \times 10^{-6}$ m/s at 333 K, and the conversions obtained in a single pass at this temperature reached over 90%. However, in most cases, an increase in the relative *p*-chlorophenol concentration is observed after a few hours of the steady-state process (this time is defined as t_s and varied among experiments), indicating a deactivation of the Pd/Fe catalyst. This phenomenon might be a consequence of several factors: pH changes in the reactor; iron hydroxide deposits on the surface of the catalyst; the loss of catalyst base through dissolution of Fe; and even catalyst flaking, which was noticed at higher temperatures. The changes in the catalyst surface at the end of the experiment, as compared to freshly prepared Pd/Fe catalyst, are evident in Figure 8.

Modeling of the observed deactivation was approached by applying the reaction kinetics with an activity term (eqs 11 and 12) to the dynamic model for a PFR. For the experimental data after the end of the steady-state

Table 1. Comparison of Reaction Rate Constant Values[a]

k (m^3/kg_{cat}·s)	catalyst, temperature	source
1.97×10^{-5}	Pd/Fe (palladized Fe plates), 293 K	PC dechlorination, this study
6.25×10^{-2}	granular Pd/Fe, 293 K	PC dechlorination[6]
3.90×10^{-4}	powdered Pd/Fe catalyst, 301 K	PC dechlorination[5]
9.30×10^{-4}	nanoscale Pd/Fe catalyst, 295 K	PCBs and TCE dechlorination[10]
9.30×10^{-5}	nanoscale Pd/Fe particles, 295 K	degradation of *trans*-DCE[12]
9.30×10^{-7}	microscale iron particles, 295 K	degradation of *trans*-DCE[12]

[a] Abbreviations: PC = *p*-chlorophenol, PCBs = polychlorinated biphenyls, TCE = trichloroethene, DCE = dichloroethene.

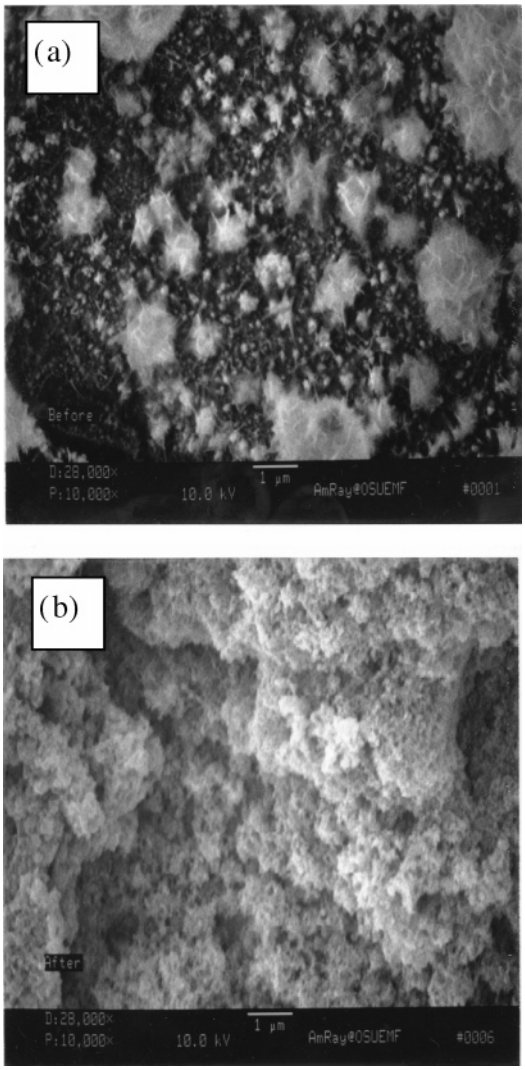

Figure 8. Comparison of SEM pictures of a Pd/Fe catalyst surface (a) before and (b) after use in the dechlorination process. The changes in the surface indicate the deposition of iron hydroxide, which presumably deactivates the catalyst.

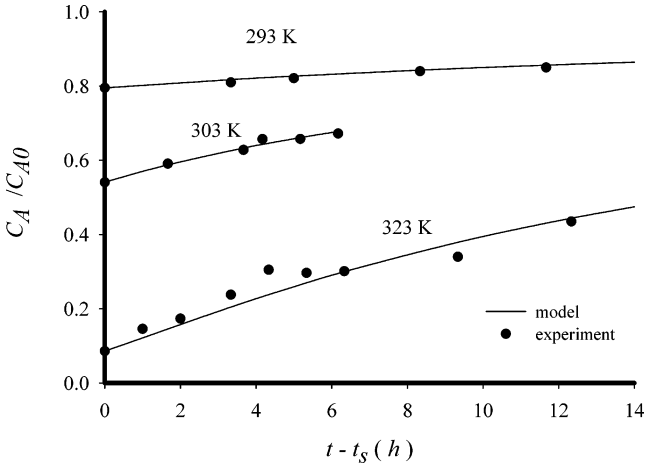

Figure 9. Experimental data on the dechlorination process at 293, 303, and 323 K and predictions of the applied model after the beginning of the deactivation process (t_s designates the process time at steady-state conditions before deactivation).

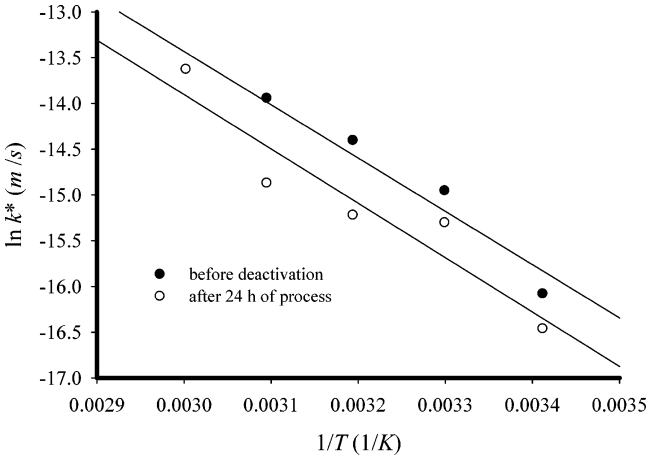

Figure 10. Calculated reaction rate constants, obtained from experimental data in the steady-state phase before catalyst deactivation (●) and after 24 h (○) of continuous processing, as a function of temperature.

phase of the continuous process (after time t_s), the reduction of catalyst activity is described as a second-order process ($n = 2$ in eq 12). The evaluated values for the deactivation rate coefficient k_d are 0.0409, 0.094, and 0.164 h^{-1} for processes at 293, 303, and 323 K, respectively. Figure 9 shows the experimental data at 293, 303, and 323 K and the applied model after the beginning of the deactivation process.

Figure 10 presents the temperature dependence of the experimental overall rate constant, determined during a steady-state phase before catalyst deactivation and after 24 h of continuous processing. Upon application of the Arrhenius law, the calculated activation energy for the steady-state conditions is $E_a = (48.43 \pm 6.13) \times 10^3$ J/mol, and the preexponential factor is $k_0 = 57.14$ m/s, whereas at the end of the experiments, $E_a = (49.39 \pm 9.71) \times 1010^3$ J/mol and $k_0 = 50.37$ m/s. We can conclude that catalyst deactivation changed the preexponential factor, while leaving the activation energy nearly the same. The E_a values found are in the same range as those reported for the hydrodechlorination of *p*-chlorophenol over Pd/C catalyst[2], but twice as high as those obtained for the hydrodechlorination of *p*-chlorophenol over Pd/ACC catalyst[3].

Conclusions

Dechlorination of *p*-chlorophenol was achieved on a Pd/Fe catalyst in a single-pass microreactor system. A 2D model, developed for this specific system, accurately predicts the experimental conversions and enables the

calculation of overall reaction rate constants. Comparison of the model simulations with ideal reactor predictions effectively shows PFR behavior at the operating conditions applied in the experiments.

The experimental results indicate moderate efficiency of the catalytic reaction in a microreactor system at room temperature. Increased temperatures resulted in higher conversions and overall reaction rate constants, although they are up to 3 orders of magnitude lower than those reported for granular and nanoscale Pd/Fe catalyst. Moreover, the deactivation of the catalyst was observed after a few hours of steady-state continuous processing and was described as a second-order process. Passivation of the catalyst resulted in a lower Arrhenius preexponential factor for the dechlorination process compared to the initial rates. The application of recent advances in microfabrication techniques for catalytic reactors would probably ensure a more stable catalyst and therefore diminish undesirable deactivation.

Acknowledgment

The authors thank Dr. Igor Plazl from Department of Chemical Engineering, Faculty of Chemistry and Chemical Technology, University of Ljubljana, Ljubljana, Slovenia, for his help in modeling and data analysis. P.Ž.P. was supported through Grant P2-0191 Chemical Engineering, provided by the Ministry of Education, Science and Sport of the Republic of Slovenia.

Nomenclature

a = catalyst activity
B = half-height of the reactor (m)
C_A = concentration of *p*-chlorophenol (mol/m^3)
C_{A0} = input concentration of *p*-chlorophenol (mol/m^3)
C_{H^*} = concentration of reactive intermediate H* in solution (mol/m^3)
D_{AB} = diffusion coefficient of *p*-chlorophenol in water (m^2/s)
d_e = equilibrium length (m)
E_a = activation energy (J/mol)
F = flow rate (m^3/s)
k = reaction rate coefficient for *p*-chlorophenol dechlorination (m^3/kg$_{cat}$·s)
k' = reaction rate coefficient for dechlorination based on the amount of catalyst (m^6/mol·kg$_{cat}$·s)
k'' = normalized reaction rate coefficient for *p*-chlorophenol dechlorination (m^3/s)
k^* = reaction rate coefficient for dechlorination, normalized by the reactor cross section (m/s)
k_0 = Arrhenius preexponential factor (m/s)
k_d = deactivation rate coefficient (h^{-1})
L = catalyst length (m)
L' = length of precatalytic zone (m)
n = deactivation order
r_A = rate of *p*-chlorophenol dechlorination (mol/s)
R = ideal gas constant (J/mol)
t = time (s, h)
t_s = time of the dechlorination process at steady-state conditions, before deactivation (h)
T = temperature (K)
v_{av} = average velocity in the z direction (m/s)
v_m = maximal velocity in the z direction (m/s)
v_z = velocity in the z direction (m/s)
X = dimensionless *p*-chlorophenol concentration
X_0 = dimensionless *p*-chlorophenol concentration at the inlet to the catalytic zone, $L = 0$
W = catalyst width (m)
w_{cat} = weight of catalyst Pd (kg)

Greek Letters

μ = fluid viscosity (Pa·s)
ρ = fluid density (kg/m^3)
ξ = dimensionless axial parameter, z/B
ψ = dimensionless radial parameter, y/B

Dimensionless Groups

$Pe = v_z B/D_{AB}$
$Re = r v_{av} d_e/\mu$

Literature Cited

(1) Ramamoorthy, S.; Ramamoorthy, S. *Chlorinated Organic Compounds in the Environment*; CRC Press: Boca Raton, FL, 1997.

(2) Yuan, G.; Keane M. A. Liquid-phase catalytic hydrodechlorination of chlorophenols at 273 K. *Catal. Commun.* **2003**, *4* (4), 195 and references therein.

(3) Shindler, Yu.; Matatov-Meytal Yu.; Steintuch, M. Wet hydrodechlorination of *p*-chlorophenol using Pd supported on an activated carbon cloth. *Ind. Eng. Chem. Res.* **2001**, *40*, 3301 and references therein.

(4) Cheng, F.; Fernando, Q.; Korte, N. Electrochemical dechlorination of 4-chlorophenol to phenol. *Environ. Sci. Technol.* **1997**, *31*, 1074 and references therein.

(5) Liu, Y.; Yang, F.; Yue, P. L.; Chen, G. Catalytic dechlorination of chlorophenols in water by palladium/iron. *Water Res.* **2001**, *35*(8), 1887 and references therein.

(6) Graham, L. J.; Jovanovic, G. Dechlorination of *p*-chlorophenol on a Pd/Fe catalyst in a magnetically stabilized fluidized bed; Implications for sludge and liquid remediation. *Chem. Eng. Sci.* **1999**, *54*, 3085 and references therein.

(7) Grittini, C.; Malcolmson, M.; Fernando, Q.; Korte, N. Rapid dechlorination of polychlorinated biphenyls on the surface of a Pd/Fe bimetallic system. *Environ. Sci. Technol.* **1995**, *29* (11), 2829.

(8) Doyle J. G.; Miles, T. A.; Parker, E.; Cheng, I. F. Quantification of total polychlorinated biphenyl by dechlorination to biphenyl by Pd/Fe and Pd/Mg bimetallic particle. *Microchem. J.* **1998**, *60* (3), 290.

(9) Neurath, S. A.; Ferguson, W. J.; Dean, S. B.; Foose, D.; Agrawal, A. Rapid and complete dehalogenation of chlorinated phenols by Fe−Pd bimetallic reductants in bench-scale reactors: Implications for soil and ground water remediation. In *213th ACS National Meeting Book of Abstracts*; American Chemical Society: Washington, DC, 1997; Paper ENVR-176.

(10) Wang, C. B.; Zhang, W. X. Synthesizing nanoscale iron particles for rapid and complete dechlorination of TCE and PCBs. *Environ. Sci. Technol.* **1997**, *31* (7), 2154.

(11) Graham, L. J. Dechlorination of *p*-chlorophenol on bimetallic Pd/Fe catalyst in a magnetically stabilized fluidized bed: Experiment and theory. Ph.D. Thesis, Oregon State University, Corvallis, Oregon, 1999.

(12) Zhang, W. X.; Wang, C. B.; Lien, H. L. Treatment of chlorinated organic contaminants with nanoscale bimetallic particles. *Catal. Today* **1998**, *40*, 387.

(13) Sakrittichai, P. Dechlorination of *p*-Chlorophenol on a Palladium Based Metal Support Catalyst in a Microreactor: Experiment and Theory. M.S. Thesis, Oregon State University, Corvallis, Oregon, 2001.

(14) Jähnisch, K.; Hessel, V.; Löwe, H.; Baerns, M. Chemistry in microstructured reactors. *Angew. Chem., Int. Ed.* **2004**, *43*, 406.

(15) Jensen, K. F. Microreaction engineering—Is small better? *Chem. Eng. Sci.* **2001**, *56* (2), 293.

(16) Swenson, E. R.; DeWitt, H. S.; Lin, J.; Hamilton, T.; Emerich, C. Combinatorial chemistry in microfluidic chips. In *Innovation and Perspectives in Solid-Phase Synthesis & Combinatorial Libraries: Peptides, Proteins and Nucleic Acids—Small Molecule Organic Chemistry Diversity, 6th International Symposium, Collected Papers*; Mayflower Scientific Ltd.: Kingswinford, U.K., 2001; p 113.

(17) Kuila, D.; Nagineni, V. S.; Potluri, A.; Zhao, S.; Aithal, R. K.; Liang, Y.; Fang, J.; Nassar, R.; Siriwardane, U.; Naidu, S. V.; Palmer, J. Microreactors for catalysis. In *Abstracts of Papers of*

the 226th ACS National Meeting; American Chemical Society, Washington, DC, 2003; Paper INOR-022.

(18) Ajmera, K. S.; Delattre, C.; Schmidt, A. M.; Jensen, K. F. Microreactors for measuring catalyst activity and determining reaction kinetics. *Stud. Surf. Sci. Catal.* **2003**, *145*, 97.

(19) Schouten, J. C.; Rebrov, E. V.; de Croon, M. H. J. M. Miniaturization of heterogeneous catalytic reactor: Prospects for new developments in catalysis and process engineering. *Chimia* **2002**, *56*, 627.

(20) Honicke, D. Microchemical reactors for heterogeneously catalyzed reactions. *Stud. Surf. Sci. Catal.* **1999**, *122*, 47.

(21) Wiessmeier G.; Honicke, D. Microfabricated components for heterogeneously catalysed reactions. *J. Micromech. Microeng.* **1996**, *6*, 285.

(22) Maruyama, T.; Uchida, J.; Ohkawa, T.; Futami, T.; Katayama, K.; Nishizawa, K.; Sotowa, K.; Kubota, F.; Kamiyaa, N.; Goto, M. Enzymatic degradation of *p*-chlorophenol in a two-phase flow microchannel system. *Lab-on-a-Chip* **2003**, *3*, 308.

(23) Wilke, C. R.; Chang, P. C. Correlation of Diffusion Coefficients in Dilute Solutions. *AIChE J.* **1955**, *1*, 164.

(24) Levenspiel, O. *Chemical Reaction Engineering*, 3rd ed.; John Wiley & Sons: New York, 1999.

(25) Deshmukh, S. R.; Mhadeshwar, A. B.; Vlachos, D. G. Microreactor modeling for hydrogen production from ammonia decomposition on ruthenium. *Ind. Eng. Chem. Res*. **2004**, *43*, 2986.

Received for review June 9, 2004
Revised manuscript received October 7, 2004
Accepted October 11, 2004

IE049496+